Characterization by electron microscopy of dimeric Photosystem II core complexes from spinach with and without CP43

Camiel Eijckelhoff [a], Jan P. Dekker [a, *], Egbert J. Boekema [b]

[a] *Department of Physics and Astronomy, Institute of Molecular Biological Sciences, BioCentrum Amsterdam, Vrije Universiteit, De Boelelaan 1081, 1081 HV Amsterdam, The Netherlands*
[b] *Department of Biophysical Chemistry, BIOSON Research Centre, University of Groningen, Nijenborgh 4, 9747 AG Groningen, The Netherlands*

Abstract

Dimeric associations of the D1-D2-CP47 and D1-D2-CP47-CP43 complexes of Photosystem II from spinach were isolated and purified with sucrose density gradient centrifugation and gel filtration chromatography and analyzed by electron microscopy and image analysis. Images of both preparations show characteristic details in protein density. The location of the CP43 subunit and the way the dimers are associated could be determined from a comparison between diamond-like monomeric projections of the D1-D2-CP47-CP43 complex (maximal dimensions along the diagonals 10–12 and 7–8 nm) and triangle-like monomeric projections of the D1-D2-CP47 complex (dimensions 8–9 and 7–8 nm). Both isolated complexes have different dimeric configurations than observed before in several other dimeric complexes, and based on biochemical considerations we conclude that both newly observed configurations are artificial. The observation of the artificial aggregates, however, allows conclusions on the organization of Photosystem II in two-dimensional crystals and on the size of the monomeric unit. We propose a model for the location of D1, D2, CP43 and CP47 in the Photosystem II core complex in which CP43 and CP47 are positioned at the tips of the monomeric unit, closely connected to D2 and D1, respectively. © 1997 Elsevier Science B.V.

1. Introduction

Photosystem II of higher plants, algae and cyanobacteria uses energy from (sun)light to catalyze the oxidation of water to molecular oxygen and the reduction of plastoquinone to plastoquinol. It consists of the so-called reaction center, where the photochemical reactions take place, a '33 kDa'-subunit shielding the water-splitting Mn-complex and two chlorophyll *a* binding proteins with apparent masses of 43 and 47 kDa (CP43 and CP47, respectively), which serve as an intrinsic antenna system. The reaction center itself consists of two large membrane spanning proteins, called D1 and D2 (apparent masses 34 and 32 kDa, respectively), as well as a heterodimeric cytochrome *b*-559 protein and some very small additional proteins with unknown functions [1].

Abbreviations: Cyt, cytochrome; DM, *n*-dodecyl-β,D-maltoside; EM, electron microscopy; HPLC, high-performance liquid chromatography; LHC, light-harvesting complex; OGP, *n*-octyl-β,D-glucopyranoside; PEG, polyethylene glycol; PS II, Photosystem II; RC, reaction center

* Corresponding author. Fax: +31 20 4447899; E-mail: dekker@nat.vu.nl

Specific for the PS II core complex from higher plants is its association with several copies of the trimeric peripheral light harvesting complex LHCII and a set of additional chlorophyll-protein complexes containing both chlorophyll *a* and *b* [2]. This contrasts with the situation of the PS II complex in cyanobacteria, where no chlorophyll *a/b* binding antenna proteins are observed, but where instead phycobiliproteins occur that form the so-called phycobilisomes.

Electron microscopy in combination with image analysis has widely been applied to study the structure of Photosystem II at low resolution. Structural information has been obtained from isolated, dimeric PS II core complexes [3–6], isolated dimeric complexes with associated peripheral antenna proteins [7,8], two-dimensional crystals prepared from detergent-solubilized PS II core [9] and CP47-D1-D2-Cyt *b*-559 complexes [10,11], and regular arrays in PS II membranes [12–17]. With this technique resolutions have been obtained down to 15 Å, which is sufficient to indicate the location of individual subunits larger than 10 kDa in size.

The location of the subunits in the PS II core complex has been tentatively assigned (see, e.g., [18], and references therein). However, because the D1, D2, CP47 and CP43 proteins form a tight complex the assignment of these proteins to the different densities in the reconstructed images is not straightforward. In addition, dimeric associations in isolated particles are sometimes suspected to be the result of salt or detergent induced aggregation [15], and also the size of the monomeric unit in regular two-dimensional arrays is not always easily determined. In view of all these uncertainties, there is quite some disagreement on the shape and size of the monomeric unit of the PS II core complex. In some studies, the top view of the monomeric unit is suggested to have a diamond-like shape with four main stain-excluding density regions and dimensions (maximal distances along the diagonals) of about 10–12 and 7–8 nm [6–8,16–18]. Tsiotis et al., however, suggested that each monomeric unit in two-dimensional crystals consists of *two* diamond-like shapes each with dimensions of about 9–10 and 6.5–7 nm [9], and that the total monomeric unit is a much larger diamond-like shape with pronounced stain accumulation in the middle and with dimensions of about 16 and 11 nm.

Nicholson et al. [15] also suggested a larger monomeric unit in two-dimensional crystals with much stain accumulation in the central part, but with a more rectangular shape and dimensions of about 18 and 14 nm.

Taken together, the shape and size of the dimeric unit of the PS II core complex observed in some studies [6–8,16–18] resembles more or less the shape and size of the monomeric complex in some other studies [9,13,15]. In the interpretation of the latter studies, however, inclusion of part of the peripheral antenna in the two-dimensional arrays can not be excluded. In the former studies, the two monomeric units show rotational symmetry towards the center of the dimer.

In this paper, we present an analysis by electron microscopy of a dimeric PS II core preparation and of a dimeric PS II core preparation depleted of the CP43-subunit. These complexes have been purified after relatively rigorous detergent treatment, and we show that these complexes are associated in different ways than in previously analyzed dimeric PS II complexes. The results are only compatible with the notion that the monomeric unit of the PS II core complex has a diamond-like shape with dimensions of about 10–12 and 7–8 nm, and that the larger subunits are dimeric complexes with or without attached light-harvesting complexes.

2. Materials and methods

CP47-RC complexes were isolated from PS II membranes as described in [19]. In short, spinach PS II membranes [20] were solubilized by *n*-octyl-β,D-glucopyranoside (OGP), after which a high-salt treatment was performed to precipitate LHCII [21]. This precipitate was removed by centrifugation, and the oxygen-evolving PS II core complexes in the supernatant were collected by subsequent precipitation with polyethylene glycol (PEG). The precipitate was washed with 0.8 M Tris-HCl (pH 8.3) to remove the extrinsic 33 kDa polypeptide, after which the pellet was resolubilized with *n*-dodecyl-β,D-maltoside (DM) and subjected to FPLC ion-exchange chromatography at 22°C to separate the CP47-RC complex from the CP43 and other contaminating complexes. For some

isolations, the separation was performed at lower temperatures (16°C), under which conditions some of the complexes retained the CP43 protein (full release of CP43 can only be obtained by prolonged incubation at temperatures of 22°C or higher [22]).

For further purification, the fraction containing the CP47-RC (or CP47-CP43-RC) complex was immediately after the ion-exchange chromatography cooled to 4°C and layered on a discontinuous sucrose density gradient composed of sucrose solutions in 20 mM BisTris, 20 mM NaCl and 10 mM $MgCl_2$ at pH 6.5 (BT buffer) + 0.03% DM containing 25-20-18-16-13-8% (w/v) sucrose, respectively. The centrifuge tubes had a volume of 12 ml and were loaded with 200 to 300 μl sample. They were centrifuged overnight at 4°C using a swing-out rotor (Beckmann, TST41) at 40 000 r.p.m. After centrifugation, particles were found in two bands in the 18 and 20% sucrose layers. Fractions in the 20% layers were further purified by gel filtration chromatography as described in [23].
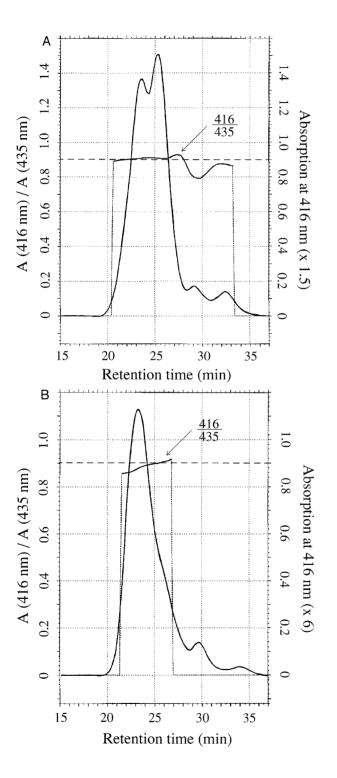
For EM, material was prepared using the droplet method with 2% uranyl acetate as the negative stain. During the staining procedure the grid was washed once with distilled water for several seconds to reduce detergent aggregation in the background. EM was performed with a JEOL JEM 1200-EX electron microscope using 80 kV at 60 000 × magnification. Micrographs were digitized with a Kodak Eikonix Model 1412 CCD camera with a step size of 22 μm, corresponding to a pixel size of 0.4 nm at the specimen level. Image analysis was carried out on a Silicon Graphics Iris work station, using IMAGIC software. From 19 micrographs about 2000 top-view projections were selected in a format of 64 × 64 pixels. Essentially we followed the alignment strategy and further analysis methods as used previously [6,24]. First the images were pretreated to normalize the variance and windowed with a circular mask. A band-pass, suppressing the highest and lowest frequencies of the images, was imposed on the particles in the alignment step. In the next steps of the image analysis procedure, the projections were rotationally and translationally aligned with correlation methods. The aligned projections were treated with multivariate statistical analysis in combination with classification [6,25]. In the classification step, 10% of the images was automatically rejected. Finally, sums of projections belonging to the various classes were made by adding the original images without band-pass filter. For these final sums, the best 50–70% of the class-members were taken, with the correlation coefficient in the alignment procedure as the quality criterion.

3. Results

The original aim of the work described below was to reinvestigate the aggregation state of CP47-RC complexes isolated according to the method of [19], or of a mix of CP47-RC and PS II core complexes when the isolation and purification procedures were carried out at 16°C. We therefore subjected these preparations to gel filtration chromatography. With the techniques developed and applied for PS II RC complexes in [23], we found for pure CP47-RC complexes a first (usually minor) peak at 23.5 min and a second peak at 25.3 min (Fig. 1A, flow rate 25 ml/h). The relative heights of both peaks varied considerably for different isolations. The particles in both peaks showed a A_{416}/A_{435} ratio of 0.92 (Fig. 1A), the expected ratio for CP47-RC complexes [23]. This result suggests that CP47-RC complexes isolated according to [19] consist of a mixture of monomeric and dimeric aggregation forms.

In order to separate these putative aggregation forms, we applied sucrose density gradient centrifugation. Analysis of the 18 and 20% sucrose layers by the gel filtration technique revealed that the two types of particles were separated to a considerable extent: the 20% layer was enriched in complexes eluting after 23.5 min, the 18% layer was enriched in complexes eluting after 25.3 min, in agreement with the tentative conclusion that the particles in the 18 and 20% sucrose layers represent monomeric and dimeric forms of the CP47-RC complex, respectively. For preparations containing a mix of CP47-RC and PS II core complexes, the chromatogram of the 20% layer did not show a constant A_{416}/A_{435} ratio and in addition showed a slightly shorter elution time of 23.2 min (Fig. 1B). At 22 min the ratio was as low as 0.86, a value expected for the PS II core complex. We tentatively conclude that the largest fractions in this particular preparation are enriched in dimeric PS II core complexes.

For analysis with EM, the complexes collected in the 20% sucrose layers were purified by gel filtration chromatography. To get concentrated samples, a flow rate of 40 ml/h was applied. In order to avoid contamination with monomeric complexes, the sample for EM was collected on the left-hand side of the main peak between 14 and 14.5 min. This corresponds with 22.4–23.2 min at a flow rate of 25 ml/h, as applied in Fig. 1A,B. In case of the preparation shown in Fig. 1B, the sample collected for EM was therefore enriched in the relatively large dimeric PS II core complexes. We note that for the analysis with EM we only used complexes that had been purified with gel filtration chromatography only minutes before use. This was necessary, because prolonged incubation led to a single peak in the chromatogram at 25.3 min, in agreement with the monomer/dimer hypothesis and suggesting that at room temperature the (putative) dimers are relatively unstable and readily dissociate into monomers.

In Fig. 2 an electron micrograph is shown from which high-contrast projections of particles in top-view position could be selected. After selection, projections were aligned and treated with multivariate statistical analysis, followed by classification. During the classification the data set, consisting of CP47-RC as well as PS II core complexes, was decomposed into 20 different classes. The procedure resulted in 15 clear class averages (Fig. 3), belonging to four different types of top-views. All projections have a dimer-like appearance. In order to analyze whether there is true symmetry or pseudo-symmetry in these projections, we applied the Fourier-ring correlation method [26] and found no evidence for pseudo-symmetry. For instance, the resolution of class images 3K-O was 20 Å, irrespective of rotating half of the images by 180 degrees. The class images 3A–E, 3F–H, 3I–J and 3K–O were combined and symmetrized into Fig. 4A, Fig. 4B, Fig. 4C and Fig. 4D, respectively.

We attribute two types of projections (Fig. 4A and

Fig. 1. A: FPLC gel filtration chromatogram recorded at 416 nm of an isolated CP47-RC complex. The chromatogram is plotted together with the A_{416}/A_{435} ratio, which was calculated with an absorbance threshold of 0.05. B: FPLC gel filtration chromatogram recorded at 416 nm of the 20% sucrose layer harvested from the sucrose density gradient of a preparation containing a mix of CP47-RC and PS II core complexes. The chromatogram is plotted together with the A_{416}/A_{435} ratio, which was calculated with an absorbance threshold of 0.05.
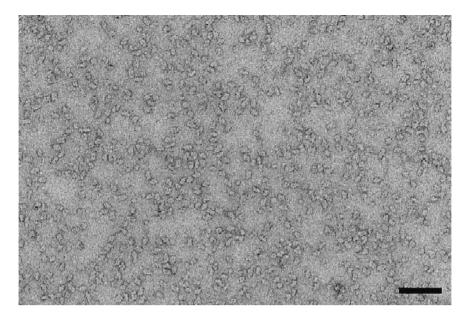
Fig. 2. Electron micrograph showing CP47-RC dimers in top-view position. Samples were prepared on carbon coated grids and negatively stained with a 2% uranyl acetate solution. The bar corresponds to 100 nm.
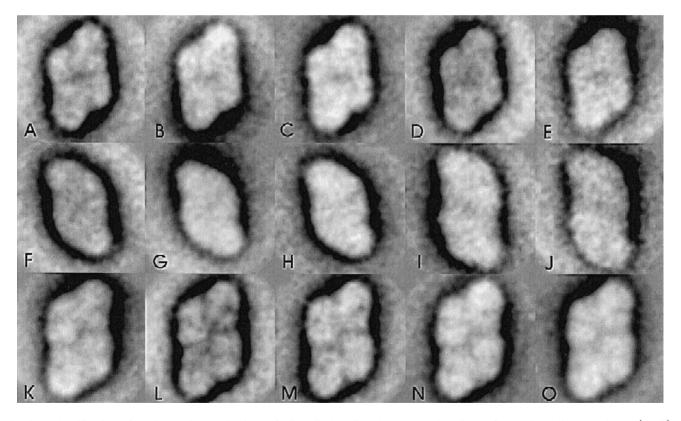

Fig. 3. A classification of 1978 top-view projections of PS II CP47-RC and core complex dimers from spinach into 15 classes (A–O). The number of projections for each group was: A: 94; B: 92; C: 103; C: 95; E: 62: F:112; G: 110; H:103; I: 67; J: 48; K: 102; L: 86; M: 81; N: 107; and O: 137, respectively. 10% of the projections were rejected during classification and five other fuzzy classes have been omitted for presentation purposes. No symmetry has been imposed on the images during analysis.
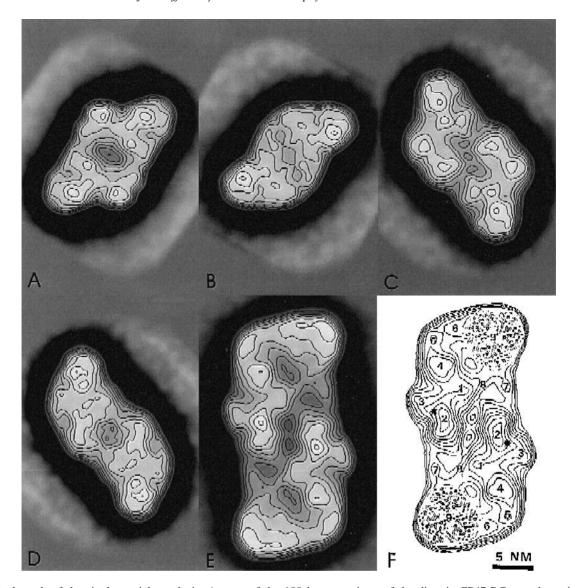
Fig. 4. Final result of the single particle analysis. A: sum of the 180 best top-views of the dimeric CP47-RC complexes in flip-type projection. B: sum of the 150 best top-views of the dimeric CP47-RC complexes in flop-type projection. To facilitate comparison, the image has been mirrored after analysis. C: sum of the 140 best top-views of dimeric core complexes in the flip-position. D: sum of the 95 best top-views of dimeric core complexes in the flop-position. To facilitate comparison, the image has been mirrored after analysis. E: image of the supercore complex, taken from [8]. F: projected structure of the PS II supercomplex in a contours-only version, taken from [7]. Protein densities have been indicated by numbers 1–4 for the part occupied by the PS II core complex and 5–9 for the major and minor LHC II antenna proteins. On density 9, the high-resolution structure of trimeric LHC II [33] has been superimposed. All images in this figure are represented with imposed two-fold symmetry.

Fig. 4B) to dimeric CP47-RC complexes in two positions on the carbon support film, flip- and flop-type, respectively. Ideally, a pure mirror-symmetric relation should exist between the projections of Fig. 4A and 4B. However, negative staining often weakens this relation, because usually the protein parts closest to the carbon support film are more strongly embedded (see [27] for a clear example). It is also possible that the protein is slightly more tilted in one position on the film than the other, which gives the projection a slimmer appearance. The images show an area of low electron density in the center. On both

sides of the center three masses can be distinguished which presumably represent the D1, D2 and CP47 proteins, in agreement with the loss of CP43.

For the particular case of the sample that contained a mixture of complexes that were and were not depleted of CP43, we would like to stress that the analysis is more sensitive for larger particles, which will therefore be selected preferentially. The images obtained for these large particles can be used for a direct comparison with the CP47-RC complexes, which makes location of the CP43 protein complex possible. The projections of Fig. 4C and 4D are attributed to PS II core particles, because the projections are slightly larger than the CP47-RC projections, and in a similar way as for the CP47-RC particles two projections are observed differing in handedness. In Fig. 4C two sets of four masses can be distinguished, which presumably represent the D1, D2, CP43 and CP47 proteins. The images have dimensions comparable to previously published ones [7], but show slight differences in the electron densities. The resolution of the images of Fig. 4A and 4B is about 25 Å, while that of the images in Fig. 4C and 4D is lower, due to a smaller number of projections.

4. Discussion

4.1. Association of monomers in dimeric units

From the comparison of spinach PS II dimers with oxygen-evolving capacity and 2D-crystals of PS II particles lacking both the 43-kDa and the 33-kDa subunit, it was already concluded that the CP43 subunit is located at the tip of the PS II dimer [6]. In this paper, we present a more direct comparison of two PS II dimers with and without CP43, which were purified and studied with EM in the same way. The images of both preparations show a detailed density structure from which conclusions can be drawn on the location of the CP43 subunit and on the way the dimers are associated.

The 'supercomplex' of PS II and LHCII [7,8] is the largest complex of PS II that has been studied with EM and single particle analysis (Fig. 4E and 4F). Because this preparation was obtained using a relatively mild isolation procedure, we would like to

refer to it as model for the in vivo situation. Thus, in the following we first adopt the dimer hypothesis [6–8,12,16–18] and then show that the results described in this paper can only be explained within the context of this hypothesis.

In [12] the four protein densities in a monomeric unit of the PS II core, which largely represent the D1, D2, CP43 and CP47 proteins according to the dimer hypothesis, were indicated by the numbers 1–4. This way of numbering was also used in [7,18] and is followed in this paper as well. In order to facilitate comparison, we have drawn a zigzag through the densities, connecting them in the order: 4-1-3-2 (Fig. 5A). In doing so we found that the shortest distances exist between the numbers 2 and 3 densities and the numbers 1 and 4 densities, while the numbers 1 and 3 densities are relatively far apart. The configuration of the monomeric protein complex shows a characteristic diamond shape. More detailed observation reveals that the four sides of the diamond show clear differences. The side between the number 1 and 4 densities is rather straight, while those between densities 1 and 2 and densities 2 and 3 are moderately curved. The side between densities 3 and 4, finally, is strongly curved to the inside of the complex (Fig. 5A). This gives the monomer a distinct a-symmetric shape, which makes comparison with monomeric units in projections of other preparations possible. In Fig. 5A it can also be seen that two monomers form a dimer in such a way that their numbers 1 and 2 densities and 2 and 1 densities, respectively, are in close contact.

The monomeric half of the image of the PS II core complex in the flip-position, as presented in Fig. 4C, also shows four more or less distinct protein densities that can be connected by a zigzag. By comparing the shape of the monomeric unit in this preparation with that described above for the supercomplex, we have assigned the numbers 1 to 4 to the different densities (Fig. 5B). The contours and the configuration of the zigzag are very similar. However, the way in which the dimer is composed of two monomeric units is completely different, because now the strongly curved side is observed at the inside of the dimer. Thus, in this preparation the dimer contact is formed by the numbers 3 and 4 densities and 4 and 3 densities, respectively. If the association of the number 1 and 2 densities observed in the spinach supercomplex [7],

spinach core dimer [6,7,28] and *Synechococcus* PS II dimer [7] is regarded as the in vivo organization, then the association involving the numbers 3 and 4 densities observed in this paper must be regarded as artificial.

The monomeric half of the image of the CP47-RC complex in the position as shown in Fig. 4A shows only three protein densities, which is in agreement with the loss of CP43. In order to facilitate comparison, we connected the three centers of highest density by lines which form an L-shape (Fig. 5C). The longest distance is that between the protein densities on the inside of the dimer, this coincides with the number 1 and 3 densities described in the previous paragraph. The protein on the outside of the dimer can therefore either be number 2 or number 4. The curved shape of the contour between this protein and the protein on the inside, suggests that this protein should be labelled number 2. An assessment can also be made by superimposing the monomeric CP47-RC unit, or its mirror image, on that of the core preparation. Although there are several different ways to do this, there is only one unique way in which the distinct monomeric shape will give a perfect fit. The result of this fit is shown in Fig. 5B, where the contours of the CP47-RC monomer are drawn onto that of the monomeric unit of the core preparation. The numbering reveals that the dimeric contact in the CP47-RC complex is formed by the numbers 1 and 3 densities and 3 and 1 densities, respectively. We therefore conclude that this complex is also an artificial dimer, but with a different configuration to that of the PS II core dimer described in the previous paragraph. The somewhat triangular shape of the complex clearly resembles that of the recently reported monomeric unit of 2D-crystals of the CP47-RC complex [11]. In these crystals, however, the number 2 density seems more pronounced than in the isolated dimers.

Work on other PS II preparations can also be discussed in terms of dimeric configurations. The 2D-crystals of the PS II core complex presented in [16], for instance, show 1 and 2 with 2 and 1, as well as 3 and 4 with 4 and 3 contacts. The first configuration is held responsible for the formation of the dimeric unit cell and corresponds with the in vivo situation as proposed in [18]. The second type of contact is obviously necessary to obtain a stable crystal, and it is remarkable that a very similar type

of configuration is found in our 'artificial' dimeric PS II core preparation.

This interpretation, however, contrasts that presented in [9]. Here the unit cell is regarded a monomer although clearly two components of similar shape can be distinguished. The contours of these components resemble those of our monomeric units, in particular in view of the deep cleft between the two densities nearest to the center (a 3 and 4 with 4 and 3 dimeric contact in our terms), although both components are about 10–20% smaller than observed in our preparations. The idea of a large monomeric unit cell was also supported in [15]. The results described in the present paper, however, are strong evidence for the dimeric model, because it is possible to explain the differences in shape between the several images (Fig. 5) assuming they represent dimers composed of two identical monomeric units in different configurations. It would be very difficult and far from unambiguous to assign these images to different monomeric configurations of the complex: it is very hard to believe that the CP47, CP43 and RC proteins would be able to form more than one type of organization. Another strong argument in favor of the dimer hypothesis is the apparent symmetry in the images with and without CP43: two protein masses are missing in the reconstructed image of the CP47-RC complex, originating from the tips of the usually observed PS II core dimer (Fig. 5A). It is highly unlikely that one CP43 protein can be responsible for both masses.

The results of the EM experiments show that it is possible to isolate 'artificial' dimers in different configurations. The artificial dimerization can possibly be explained by the pretreatments that have been used before the final isolation and purification of the particles. In particular, the treatment with *n*-octyl-β,D-glucopyranoside (OGP) that we used to remove the major Chl *a/b*-binding complex LHCII, the PEG precipitation treatment and the subsequent mild 'solubilization' with DM may have led to artificial dimeric configurations after purification of the proteins. Incomplete DM solubilization of PEG-induced aggregates may also very well explain why our dimeric configurations were found to be unstable. The PS II core dimers with the contacts between the numbers 1 and 2 densities and 2 and 1 densities [6,7,28], however, were prepared with relatively simple detergent solubilization procedures without inter-

mediate precipitation steps, are more stable, and can therefore be regarded to reflect the in vivo situation in the photosynthetic membrane. Recently, Hankamer et al. [8] presented evidence for this idea.

4.2. Subunit arrangement in monomeric units

From the above described comparison between the CP47-RC and core preparations it can be concluded that the number 4 protein density can be assigned to CP43. This is in agreement with what was concluded earlier [6]. The assignment of the other proteins in the PS II core complex, however, is less unambiguous. Up to now the D1, D2 and CP47 proteins have only roughly been assigned. This is partly due to the relatively low resolution of these masses in the images. The resolution of our images, however, does allow a qualitative comparison of the relative sizes of the observed densities.

From Fig. 4A it becomes clear that there is one relatively large mass on the outside of the monomeric half of the dimer (number 2) and that there are two masses of comparable size situated next to each other (numbers 1 and 3). The apparent masses of the D1, D2 and CP47 proteins give reason to the tentative

assignment of the number 2 density to CP47. In Fig. 4B it can be seen that densities 2 and 4, which we assign to CP47 and CP43, respectively, also have more or less the same size, which agrees with the fact that these proteins have similar masses. Biochemical evidence for the location of CP43 on the outside of the dimer can be found in the fact that this protein is relatively easy to remove compared to CP47 [19]. Furthermore, deletion of its gene (*Psb*C) does not prevent PS II assembly in vivo and it is possible to isolate PS II complexes devoid of CP43 that still retain functional secondary donor and acceptor electron transfer [29]. CP47, in contrary, is thought to play an important role in maintaining the dimeric structure. This is supported by the observation that no reaction center assembly is detected in the absence of CP47 [30] and by the lack of stability of our artificial dimers, in which CP47 is located on the outside of the dimer.

The location of the D1 protein can be speculated from a physiological point of view. It is known from biochemical experiments that there is a rapid exchange of this protein in case of damage [31]. This is easier to realize if the protein is located on the outside of the complex. Furthermore, the mobile plastoquinone molecule requires an easy passage from
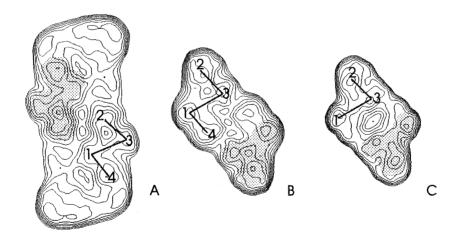

Fig. 5. A comparison of the top-view of the dimeric CP47-RC complex (C) with the dimeric supercomplex (A) and the dimeric PS II core complex (B). The data in (A) were taken from Fig. 4E. To facilitate comparison, the densities 1–4 (see Fig. 4) have been connected by zigzags and the approximate contours of the monomeric unit of the CP47-RC particle are marked in (B) and (C). In (A) the characteristic diamond shape of the monomeric unit composed of the PS II core complex is marked. In (A) the highest density does not exactly match the densities connected by the zigzag; this highest density area has been shown to be occupied by the extrinsic 33 kDa protein ([18], and E.J. Boekema, J. Nield, B. Hankamer and J. Barber, unpublished results). In the complexes presented in (B) and (C) this subunit is absent ([19]), resulting in four (B) or three (C) highest densities connected by the zigzag. In the Discussion section a model is proposed in which the four protein densities are assigned in the following way: 1, D2; 2, CP47; 3, D1 and 4, CP43.

and to a position near the center of the D1D2 complex where presumably the Q_B binding site is located (see [32] and references therein), which may be realized by the deep cleft between densities 3 and 4 (Fig. 5A). Both these conditions are satisfied when the D1 protein is located at the number 3 position in the EM-image and the D2 protein in the number 1 position. We note that in this proposal the extrinsic 33 kDa protein binds in the triangle formed by density 2 (CP47), density 3 (D1) and the center between densities 1 and 3 (the heart of the RC), and that the primary quinone Q_A would be located near the region where densities 1 (D2) and 4 (CP43) are in close contact. The positioning of CP43 may help to explain the relative stability of Q_A in the photosynthetic membrane and the instability of Q_A upon removal of the CP43 protein [22].

Concludingly, we propose a model for the complex of D1, D2, CP43 and CP47 in which the proteins have a more or less symmetrical arrangement, with the D1 and D2 proteins next to each other (number 3 and 1 positions, respectively) and the CP43 and CP47 on either side (number 4 and 2 positions, respectively). Considering the high degree of similarity in size and structure of these two pairs of proteins, this conformation is realistic. We note that this speculation is largely based on the apparent symmetry of the complex, and that in [18] another organization was favored, although the presently proposed configuration was not excluded. First results from antibody labelling [16] seem to favor the model in [18], but these particular results in [16] are not without doubt. The differences in densities between labelled and non-labelled complexes are exclusively found at the margins of the reconstructed images, and can therefore also be explained by differences in resolution. Clearly more evidence is needed to be able to reject one or both proposed models.

Acknowledgements

References

[1] B.A. Diner, G.T. Babcock, In: D.R. Ort, C.F. Yocum (Eds.), Oxygenic Photosynthesis: The Light Reactions, Kluwer Academic Publishers, Dordrecht, 1996, pp. 213–247.

[2] H. Paulsen, Photochem. Photobiol. 62 (1995) 367–382.

[3] M. Rögner, J.P. Dekker, E.J. Boekema, H.T. Witt, FEBS Lett. 219 (1987) 207–211.

[4] J.P. Dekker, E.J. Boekema, H.T. Witt, M. Rögner, Biochim. Biophys. Acta 936 (1988) 307–318.

[5] E. Haag, E.J. Boekema, K.D. Irrgang, G. Renger, Eur. J. Biochem. 189 (1990) 47–53.

[6] E.J. Boekema, A.F. Boonstra, J.P. Dekker, M. Rögner, J. Bioenerg. Biomembr. 26 (1994) 17–29.

[7] E.J. Boekema, B. Hankamer, D. Bald, J. Kruip, J. Nield, A.F. Boonstra, J. Barber, M. Rögner, Proc. Natl. Acad. Sci. USA 92 (1995) 175–179.

[8] B. Hankamer, J. Nield, D. Zheleva, E. Boekema, S. Jansson, J. Barber, Eur. J. Biochem. 243 (1997) 422–429.

[9] G. Tsiotis, T. Walz, A. Spyridaki, A. Lustig, A. Engel, D. Ghanotakis, J. Mol. Biol. 259 (1996) 241–248.

[10] J.P. Dekker, S.D. Betts, C.F. Yocum, E.J. Boekema, Biochemistry 29 (1990) 3220–3225.

[11] K. Nakazato, C. Toyoshima, I. Enami, Y. Inoue, J. Mol. Biol. 257 (1996) 225–232.

[12] M.K. Lyon, K.M. Marr, P.S. Furcinitty, J. Struct. Biol. 110 (1993) 133–140.

[13] A. Holzenburg, M.C. Bewley, F.H. Wilson, W.V. Nicholson, R.C. Ford, Nature 363 (1993) 470–472.

[14] C. Santini, V. Tidu, G. Tognon, A. Ghiretti Magaldi, R. Bassi, Eur. J. Biochem. 221 (1994) 307–315.

[15] W.V. Nicholson, F.H. Shepherd, M.F. Rosenberg, R.C. Ford, A. Holzenburg, Biochem. J. 315 (1996) 543–547.

[16] K.M. Marr, D.N. Mastronarde, M.K. Lyon, J. Cell Biol. 132 (1996) 823–833.

[17] K.M. Marr, R.L. McFeeters, M.K. Lyon, J. Struct. Biol. 117 (1996) 86–98.

[18] M. Rögner, E.J. Boekema, J. Barber, Trends Biochem. Sci. 21 (1996) 44–49.

[19] J.P. Dekker, N.R. Bowlby, C.F. Yocum, FEBS Lett. 254 (1989) 150–154.

[20] D.A. Berthold, G.T. Babcock, C.F. Yocum, FEBS Lett. 134 (1981) 231–234.

[21] D.F. Ghanotakis, D.M. Demetriou, C.F. Yocum, Biochim. Biophys. Acta 891 (1987) 15–21.

[22] J. Petersen, J.P. Dekker, N.R. Bowlby, D.F. Ghanotakis, C.F. Yocum, G.T. Babcock, Biochemistry 29 (1990) 3226–3231.

[23] C. Eijckelhoff, H. van Roon, M.-L. Groot, R. van Grondelle, J.P. Dekker, Biochemistry 35 (1996) 12864–12872.

[24] G. Harauz, E. Boekema, M. van Heel, Meth. Enzymol. 164 (1988) 35–49.

[25] E.J. Boekema, B. Böttcher, Biochim. Biophys. Acta 1098 (1992) 131–143.

[26] M. Van Heel, Ultramicroscopy 21 (1987) 95–100.

[27] B. Böttcher, P. Gräber, E.J. Boekema, Biochim. Biophys. Acta 1100 (1992) 125–136.

[28] A.F. Boonstra, Doctoral Thesis, Rijksuniversiteit Groningen, The Netherlands, 1996.

[29] M. Rögner, D.A. Chisholm, B.A. Diner, Biochemistry 30 (1991) 5387–5395.

[30] G. Shen, W.F.J. Vermaas, J. Biol. Chem. 269 (1994) 13904–13910.

[31] E.M. Aro, I. Virgin, B. Andersson, Biochim. Biophys. Acta 1143 (1993) 113–134.

[32] B. Svensson, C. Etchebest, P. Tuffery, P. van Kan, J. Smith, S. Styring, Biochemistry 35 (1996) 14486–14502.

[33] W. Kühlbrandt, D.N. Wang, Y. Fujiyoshi, Nature 367 (1994) 614–621.